Monthly Notices
of the
ROYAL ASTRONOMICAL SOCIETY

Mon. Not. R. Astron. Soc. **401,** 1465–1474 (2010) doi:10.1111/j.1365-2966.2009.15760.x

Towards the properties of long gamma-ray burst progenitors with *Swift* data⋆

Xiao-Hong Cui,[1]† En-Wei Liang,[2] Hou-Jun Lv,[2] Bin-Bin Zhang[3] and Ren-Xin Xu[1]

[1]*School of Physics and State Key Laboratory of Nuclear Physics and Technology, Peking University, Beijing 100871, China*
[2]*Department of Physics, Guangxi University, Nanning 530004, China*
[3]*Department of Physics and Astronomy, University of Nevada, Las Vegas, NV 89154, USA*

Accepted 2009 September 22. Received 2009 September 21; in original form 2009 July 6

ABSTRACT

We investigate the properties of both the prompt and X-ray afterglows of gamma-ray bursts (GRBs) in the burst frame with a sample of 33 *Swift* GRBs. Assuming that the steep decay segment in the canonical X-ray afterglow light curves is due to the curvature effect, we fit the light curves with a broken power law to derive the zero time of the last emission epoch of the prompt emission (t_1) and the beginning as well as the end time of the shallow decay segment (t_2 and t_3). We show that both the isotropic peak gamma-ray luminosity ($L_{\rm peak,\gamma}$) and gamma-ray energy ($E_{\rm iso,\gamma}$) are correlated with the isotropic X-ray energy ($E_{\rm iso,X}$) of the shallow decay phase and the isotropic X-ray luminosity at $t_2(L_{\rm X,t_2})$. We infer the properties of the progenitor stars based on a model proposed by Kumar et al. who suggested that both the prompt gamma-rays and the X-ray afterglows are due to the accretions of different layers of materials of the GRB progenitor star by a central black hole (BH). We find that most of the derived masses of the core layers are $M_{\rm c} = 0.1 \sim 5\,{\rm M}_\odot$, and their average accretion rates in the prompt gamma-ray phase are $\dot{M}_{\rm c} = 0.01 \sim 1\,{\rm M}_\odot\,{\rm s}^{-1}$, with a radius of $r_{\rm c} = 10^8 \sim 10^{10}$ cm. The rotation parameter is correlated with the burst duration, being consistent with the expectation of collapsar models. The estimated radii and the masses of the fall-back materials for the envelope layers are $r_{\rm e} = 10^{10} \sim 10^{12}$ cm and $M_{\rm e} = 10^{-3} \sim 1\,{\rm M}_\odot$, respectively. The average accretion rates in the shallow decay phase are correlated with those in the prompt gamma-ray phase, but they are much lower, i.e. $\dot{M}_{\rm e} = 10^{-8} \sim 10^{-4}\,{\rm M}_\odot\,{\rm s}^{-1}$. The $r_{\rm e}$ values are smaller than the photospheric radii of Wolf–Rayet stars. In our calculation, we assume a uniform mass of the central BH ($M_{\rm BH} = 10\,{\rm M}_\odot$). Therefore, we may compare our results with simulation results. It is interesting that the assembled mass density profile for the bursts in our sample is well consistent with the simulation for a pre-supernova star with mass $M = 25\,{\rm M}_\odot$.

Key words: radiation mechanisms: non-thermal – gamma-rays: bursts.

1 INTRODUCTION

One of the unexpected findings with the X-Ray Telescope (XRT) on-board the gamma-ray burst (GRB) mission *Swift* is the discovery of a canonical X-ray light curve, which shows successively four power-law decay segments with superimposed erratic flares (Nousek et al. 2006; Zhang et al. 2006). It starts with an initial steep decay following the prompt emission. This phase usually lasts hundreds of seconds and could be generally explained as the tail emission of the prompt GRB due to the curvature effect (Kumar & Panaitescu 2000; Qin et al. 2004; Liang et al. 2006; Zhang et al. 2006, 2009; Zhang 2007; Qin 2008). A shallow decay segment, which lasts from hundreds to thousands of seconds, is usually seen following the GRB tail (O'Brien et al. 2006; Liang, Zhang & Zhang 2007). It transits to a normal decay segment or a sharp drop (Liang et al. 2007; Troja et al. 2007).

Phenomenologically, the canonical light curves are well fitted with a two-component model (Willingale et al. 2007; Ghisellini 2008), but the physics that shapes the canonical XRT light curves is unclear (Zhang 2007). The origin of the shallow decay segment is under debate. The normal decay segments following the shallow decay segment are roughly consistent with the forward shock models (Liang et al. 2007; Willingale et al. 2007), favouring the long-lasting energy injection models for the shallow-decay segments (Zhang 2007). The chromatic transition time observed in both the X-ray and optical afterglows challenges

⋆Send offprint request to: Enwei Liang (lew@gxu.edu.cn)
†E-mail: xhcui@bac.pku.edu.cn

this scenario (Fan & Piran 2006; Liang et al. 2007; Panaitescu 2007).

Alternative models were proposed to explain the shallow decay segment(see review by Zhang 2007). The shallow decay would result in a high gamma-ray efficiency (e.g. Zhang et al. 2007a), and Ioka et al. (2006) proposed that the efficiency crisis may be avoided if a weak relativistic explosion occurs 10^3–10^6 s prior to the main burst or if the microphysical parameter of the electron energy increases during the shallow decay. Shao & Dai (2007) interpreted the X-ray light curve as due to dust scattering of some prompt X-rays (cf. Shen et al. 2009). The scattering of the external forward shock or of the internal shock synchrotron emission by a relativistic outflow could also explain the observed X-ray afterglows (Shen, Kumar & Robinson 2006; Panaitescu 2007). Uhm & Beloborodov (2007) and Genet, Daigne & Mochkovitch (2007) interpreted both X-ray and optical afterglow as emission from a long-lived reverse shock. Liang et al. (2007) argued that the physical origin of the shallow decay segment may be diverse and those shallow decay segments following an abrupt cut-off might be of internal origin (see also Troja et al. 2007). Ghisellini et al. (2007) suggested that the shallow-to-normal transition in the X-ray afterglows may be produced by late internal shocks, and the transition is due to the jet effect in the prompt ejecta (see also Nava et al. 2007). Racusin et al. (2009) also suggested that the shallow-to-normal transition may be a jet break occurring during energy injection. Interestingly, Yamazaki (2009) recently suggested that the X-ray emission might be an independent component prior to the GRB trigger. By shifting the zero time-point of the shallow-to-normal decay segment in the canonical XRT light curves, Liang et al. (2009) found that the shallow-to-normal decay behaviour might be due to a reference time effect.

It has long been speculated that long GRBs are associated with the deaths of massive stars and hence supernovae (SNe) (Colgate 1974; Woosley 1993; see Zhang & Mészáros 2004; Piran 2005; Mészáros 2006; Woosley & Bloom 2006 for reviews). The collapsar model is the most promising scenario, in which the GRB jets are powered by the accretion of an accretion disc or a torus fed by the fall-back material from the collapsar envelope (e.g. Popham, Woosley & Fryer 1999; Narayan, Piran & Kumar 2001; Di Matteo, Perna & Narayan 2002; Kohri & Mineshige 2002; Kohri, Narayan & Piran 2005; Lee, Ramirez-Ruiz & Page 2005; Gu, Liu & Lu 2006; Chen & Beloborodov 2007; Janiuk et al. 2007; Kawanaka & Mineshige 2007; Liu et al. 2007; Janiuk & Proga 2008). Kumar, Narayan & Johnson (2008a,b) proposed that the canonical light curves may be produced by the mass accretion of different layers of progenitor stars. In the framework of their model, the X-ray emission of GRBs may give insight into the properties of the progenitors. In this paper, we investigate the characteristics of the X-ray afterglow light curves in the GRB rest frame and infer the properties of progenitor stars with a sample of 33 GRBs based on the model of Kumar et al. Our sample selection and the method are presented in Section 2. In Section 3, we give the correlations between the prompt gamma-rays and the X-rays in the shallow decay segment. Inferred parameters of progenitor stars are reported in Section 4. The results are summarized in Section 5 with some discussion. Throughout, a concordance cosmology with parameters $H_0 = 71\,\mathrm{km\ s^{-1}\ Mpc^{-1}}$, $\Omega_M = 0.30$ and $\Omega_\Lambda = 0.70$ are adopted.

2 DATA

The XRT data are downloaded from the *Swift* data archive. The HEASOFT packages, including XSPEC, XSELECT, XIMAGE and *Swift* data analysis tools, are used for the data reduction. We use an IDL code developed by Zhang, Liang & Zhang (2007b) to automatically process the XRT data for all the bursts detected by Swift/BAT with redshift measurements up to 2008 October. Our sample includes only those XRT light curves that have a clear initial steep decay segment, a shallow decay segment and a normal decay segment. We get a sample of 33 GRBs. We fit the spectra accumulated in the steep and shallow segments with an absorbed power-law model and derived their spectral indices.[1] Regarding the steep decay segment as a GRB tail due to the curvature effect (e.g. Liang et al. 2006; Zhang 2007, 2009; Qin 2009), we estimate the time of last emission episode of the GRB phase with the relation $\alpha = 2 + \beta$ (Kumar & Panaitescu 2000; Liang et al. 2006). We fit the steep-to-shallow decay segment with

$$F = F_0 \left[\left(\frac{t - t_1}{t_1} \right)^{-(2+\beta_1)} + \left(\frac{t_2 - t_1}{t_1} \right)^{-(2+\beta_1)} \times \left(\frac{t}{t_2} \right)^{-\alpha_2} \right], \quad (1)$$

where t_1 is zero time-point of the last emission epoch of the prompt gamma-rays and t_2 is the starting time of the shallow decay segment. The end time of the shallow decay segment (t_3) is taken as the break time between the shallow to normal decay phases. Flares in the steep-to-shallow decay segments are removed, if any. Technically, the shallow decay segments are poorly sampled for some GRBs. We fix the α_2 value in order to get a reasonable fit. Illustrations of our fitting results for 24 bursts of our sample are shown in Fig. 1. We derive the X-ray fluence S_X in the time interval $[t_2, t_3]$ in the XRT band and calculate the isotropic X-ray energy with $E_{\mathrm{iso,X}} = 4\pi D_\mathrm{L}^2 S_\mathrm{X}/(1+z)$, where D_L is the luminosity distance. The isotropic peak fluxes of the prompt gamma-rays ($L_{\mathrm{peak},\gamma}$) are in 1024 ms time-scale. We take the X-ray luminosity at t_2, L_{X,t_2}, as a characteristic luminosity of the shallow decay segment. Our results are summarized in Table 1. With the data reported in Table 1, we show the distributions of t_1, t_2 and t_3 in comparison with GRB duration T_{90} in Fig. 2. It is found that the distribution of t_1 is comparable to T_{90}, t_2 is about 100–1000 s and t_3 is in 10^4–10^5 s.

3 CORRELATIONS

The correlations between the prompt gamma-rays and the X-rays in the shallow decay segment may reveal some physical relations between these two phases. We show the pair correlation of the observables between the two phases in Fig. 3, and measure these correlations with the Spearman correlation analysis. Our results are reported in Table 2. We find that there are several outliers at $T_{90} < 30$ s in the correlation of T_{90} and t_1. It seems natural that for long bursts t_1 could be a mark of the end of the prompt emission epoch and will be very likely approximately equal to T_{90}, since the time of the last pulse should occur close to the end of the overall emission. This breaks down for shorter bursts, where the offset between T_{90} and t_1 becomes important. We also find that T_{90} is not correlated with the time intervals $t_2 - t_1$ and $t_3 - t_2$, indicating that the break features in the XRT light curves are independent of the durations of the prompt gamma-rays. The energy releases in the two phases

[1] Although the steep decay segment has significant spectral evolution (Zhang et al. 2007b), we derive only the time-integrated spectral index for our analysis.

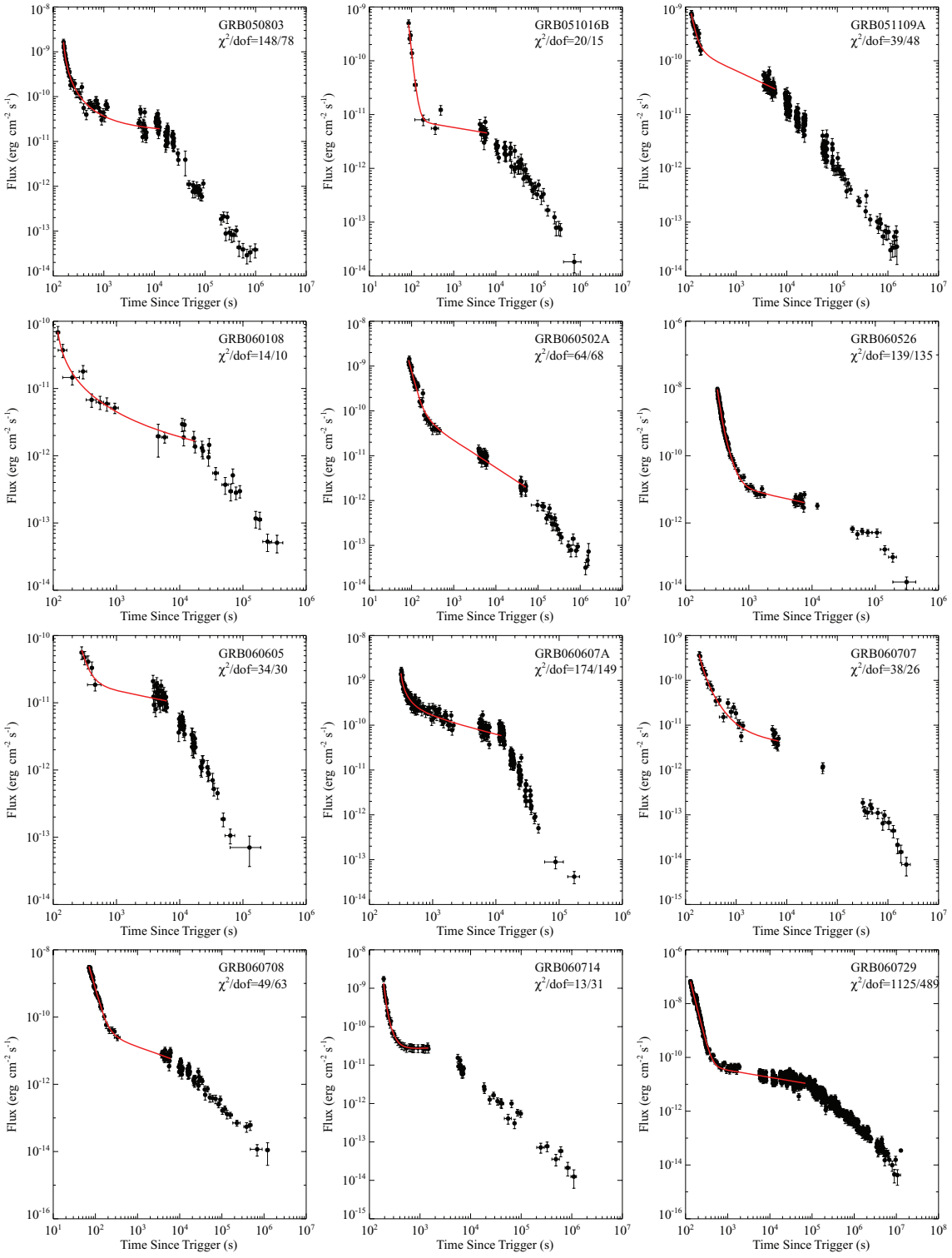

Figure 1. Illustration of the XRT light curves (dots with error bars) with our best-fitting *red solid* for some bursts in our sample. The χ^2 and degrees of freedom of the fits are also marked in each panel.

are strongly correlated. The $L_{\rm peak,\gamma}$ and $E_{\rm iso,\gamma}$ are correlated with the X-ray luminosity at $t_2(L_{\rm X,t_2})$. This fact likely suggests that the two phases may have related energy budgets from the same central engine, and the physical conditions to power the gamma-rays and the X-rays should be similar.

4 PROPERTIES OF PROGENITOR STARS

Kumar et al. (2008a,b) proposed that the prompt gamma-rays and X-ray afterglows are due to accretion of different layers of a collapsar by a newly formed black hole (BH) with 10 $M_\odot$. In their

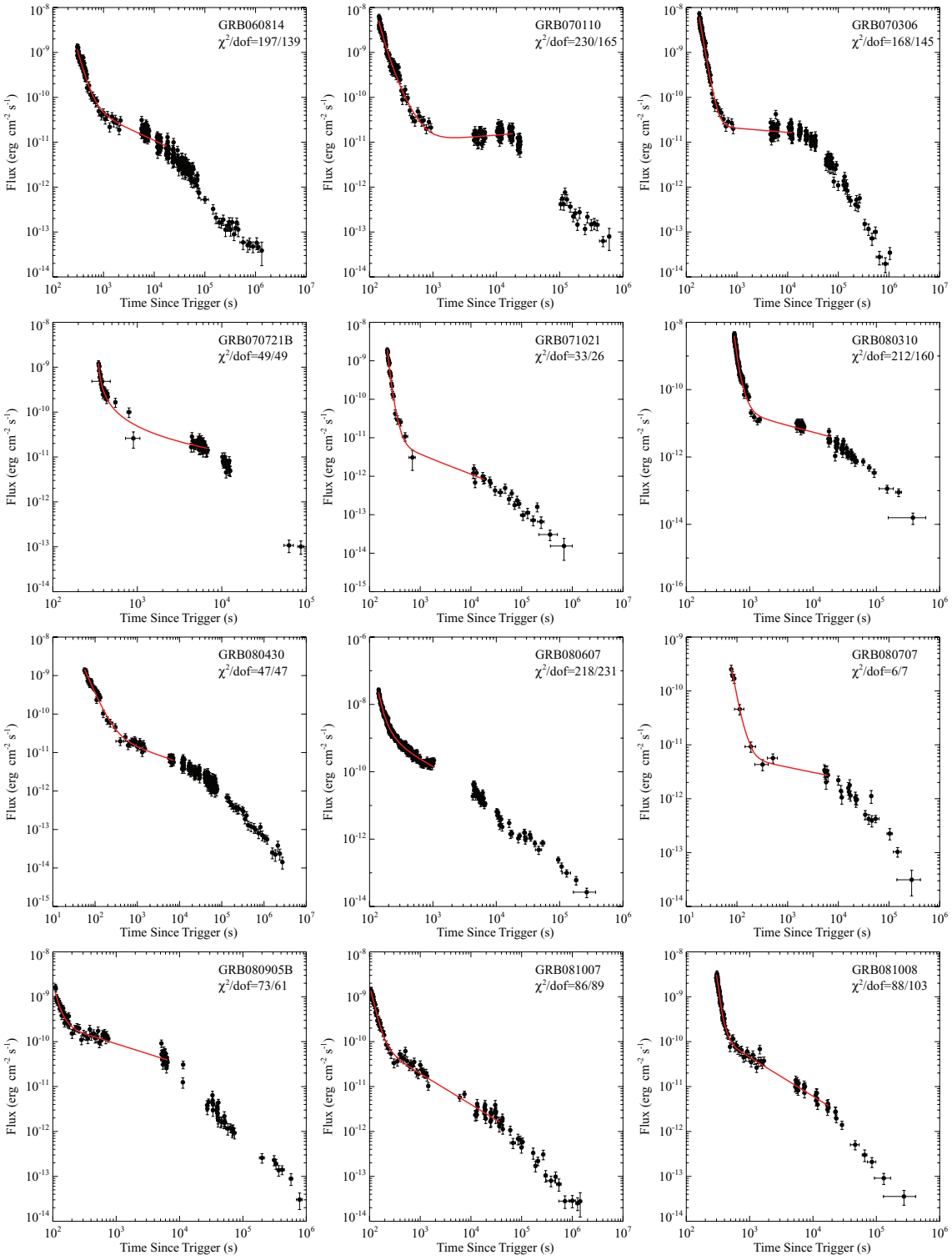

Figure 1 – *continued*

model, the highly variable light curves of the prompt gamma-rays are explained as production of the accretion of the dense, clumpy materials of the stellar core and the power-law decay X-rays may be due to the accretion of the fall-back materials of the progenitor envelope. In this section, we derive the properties of the progenitor stars based on the model of Kumar et al.

As mentioned by Kumar et al. (2008b) and from the numerical simulations from GRMHD by McKinney (2005), the efficiency of the accreted energy to the radiation is likely to depend on many details. Here, we assume a uniform radiation efficiency of 1 per cent of the accreted mass by a rotating BH (McKinney 2005). We also do not consider the beaming effect. Then, the masses accreted by the BH

Table 1. XRT Observations and our fitting results.

GRB	S_x[a] (10^{-7} erg cm^{-2})	Γ_x[b]	t_1[c] (s)	t_2[d] (s)	t_3 (ks)	α_2[e]	$E_{\rm iso,X}$ (10^{50} erg)	$L_{\rm X,t_2}$ (10^{47} erg s^{-1})
050416A	0.62 ± 0.38	2.15	$\sim$79	$\sim$87	1.74	0.70	0.7 ± 0.4	3.7
050803	5.96 ± 0.51	1.88	104 ± 5	263 ± 11	13.71	0.36	2.6 ± 0.2	0.8
050908	0.13 ± 0.11	3.90	120 ± 50	684 ± 82	8.00	1.01	2.9 ± 2.4	1.4
051016B	2.18 ± 1.10	2.82	50 ± 5	157 ± 12	6.64	0.14	4.9 ± 2.5	0.6
051109A	3.46 ± 0.75	2.33	62 ± 23	173 ± 33	7.30	0.42	42.9 ± 9.3	109.3
060108	0.53 ± 0.17	1.91	40 ± 30	186 ± 31	22.08	0.39	5.1 ± 1.6	5.4
060210	4.86 ± 0.69	1.93	298 ± 8	452 ± 11	7.00	0.80	141.0 ± 20.0	721.2
060418	1.38 ± 0.66	2.04	81 ± 2	309 ± 4	1.00	$\sim$0	7.6 ± 3.6	51.6
060502A	5.09 ± 1.19	2.43	12 ± 6	190 ± 13	72.57	0.59	28.6 ± 6.7	16.9
060510B	0.28 ± 0.27	1.42	310 ± 2	$\sim$3205	170.00	$\sim$0	11.4 ± 10.9	0.7
060522	0.12 ± 0.20	1.97	117 ± 15	248 ± 16	0.73	$\sim$0	5.2 ± 8.6	114.7
060526	0.46 ± 0.26	1.80	266 ± 1	1023 ± 18	10.00	$\sim$0	9.6 ± 5.4	9.2
060605	0.82 ± 0.52	1.60	59 ± 74	455 ± 42	7.00	$\sim$0	22.8 ± 14.5	29.3
060607A	8.45 ± 0.17	1.79	214 ± 12	384 ± 10	12.34	0.44	166.0 ± 3.3	408.0
060707	0.55 ± 0.26	2.00	56 ± 22	505 ± 76	10.00	0.39	12.8 ± 6.0	12.5
060708	0.96 ± 1.06	2.51	20 ± 2	231 ± 19	6.66	0.39	11.5 ± 12.7	16.8
060714	1.48 ± 0.46	2.02	145 ± 4	311 ± 15	3.70	0.02	23.5 ± 7.3	33.1
060729	19.58 ± 0.83	2.71	120 ± 2	425 ± 8	72.97	0.27	14.3 ± 0.6	1.0
060814	6.93 ± 0.87	1.84	81 ± 13	967 ± 74	17.45	0.15	12.5 ± 1.6	1.4
060906	0.96 ± 0.29	2.44	85 ± 26	222 ± 21	13.66	0.33	25.2 ± 7.6	20.7
061121	19.89 ± 6.14	1.62	103 ± 2	176 ± 3	2.43	0.25	85.4 ± 26.4	60.5
070110	3.59 ± 0.23	2.11	61 ± 3	522 ± 19	20.40	0.17	44.7 ± 2.9	17.2
070306	2.53 ± 0.94	2.29	110 ± 2	542 ± 8	15.00	$\sim$0	14.0 ± 5.2	4.6
070318	0.79 ± 1.45	1.40	86 ± 12	809 ± 47	2.00	$\sim$0	1.4 ± 2.6	3.2
070721B	1.80 ± 1.38	1.48	289 ± 9	450 ± 28	7.50	0.62	46.2 ± 35.4	192.2
071021	0.24 ± 0.39	2.12	175 ± 3	558 ± 74	20.00	0.37	10.1 ± 16.6	15.6
080310	1.19 ± 0.53	1.45	504 ± 1	$\sim$1313	20.00	0.33	15.7 ± 7.0	9.1
080430	0.82 ± 0.23	2.42	0 ± 5	165 ± 12	8.80	0.52	1.2 ± 0.3	2.2
080607	2.85 ± 0.81	1.81	100 ± 2	238 ± 7	1.50	1.03	54.7 ± 15.5	954.8
080707	0.24 ± 0.13	2.10	34 ± 8	192 ± 28	7.60	0.16	0.9 ± 0.5	8.4
080905B	3.50 ± 2.34	1.49	62 ± 5	179 ± 7	6.50	$\sim$0	44.4 ± 29.7	104.4
081007	0.96 ± 0.31	3.00	$\sim$35	188 ± 5	40.00	0.69	0.7 ± 0.2	1.4
081008	1.59 ± 0.52	1.91	232 ± 3	484 ± 15	20.00	0.73	14.5 ± 4.7	35.0

[a]The X-ray fluence integrated from t_2 to t_3 and its error in the XRT band (0.3–10 keV).
[b]The time-averaged photon index of the steep decay phase.
[c]The zero time of the emission epoch corresponding to the steep decay segment.
[d] t_2 and t_3 are the begin and the end times of the shallow decay segment.
[e]The slopes of the shallow decay segment.

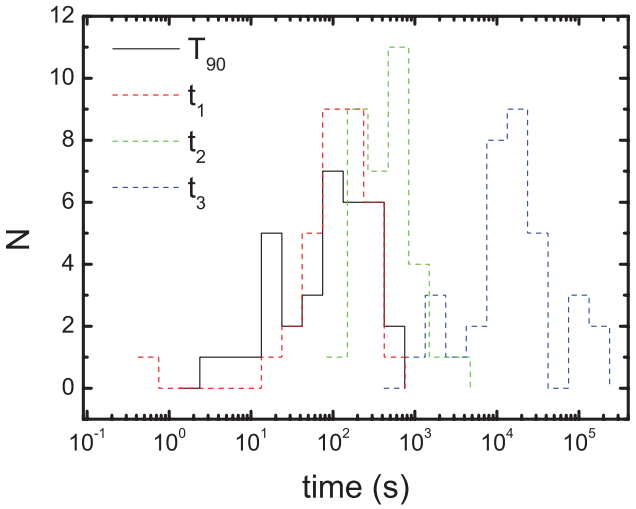

Figure 2. Distributions of logrithmic T_{90}, t_1, t_2 and t_3.

during the prompt gamma-ray phase (M_γ) and during the shallow decay phase ($M_{\rm X}$) are estimated with $M_{\rm acc} \sim 100 E_{\rm iso}/c^2$. The average accretion rate thus can be estimated with $\dot{M} \sim M_{\rm acc}/T_{\rm acc}$, where $T_{\rm acc}$ is the accretion time-scale in the rest frame. Considering the fall-back of total accreted particles as free-fall, the radius r for the fall-back time T' can be estimated with

$$r_{10} \sim 1.5 T_2^{'2/3} M_{\rm BH,1}^{1/3}, \quad (2)$$

where $r_{10} = r/10^{10}$ cm, $M_{\rm BH,1} = M_{\rm BH}/10{\rm M}_\odot$ and $T_2^{'} = T^{'}/10^2$ s. We assume $M_{\rm BH,1} = 1$ in this work. The rotation rate $f_\Omega(r)$ of the fall-back material at radius r is defined as a ratio of the local angular velocity $\Omega(r)$ to the local Keplerian velocity $\Omega_k(r)$ of the material at r:

$$f_\Omega(r) \equiv \frac{\Omega(r)}{\Omega_k(r)}. \quad (3)$$

Considering the viscosity among accreted particles before they reach the BH and combining with equation (2), one can obtain

$$f_\Omega(r) \propto \left(\frac{t_{\rm acc}\alpha_{\rm vis}}{10T'}\right)^{1/3}, \quad (4)$$

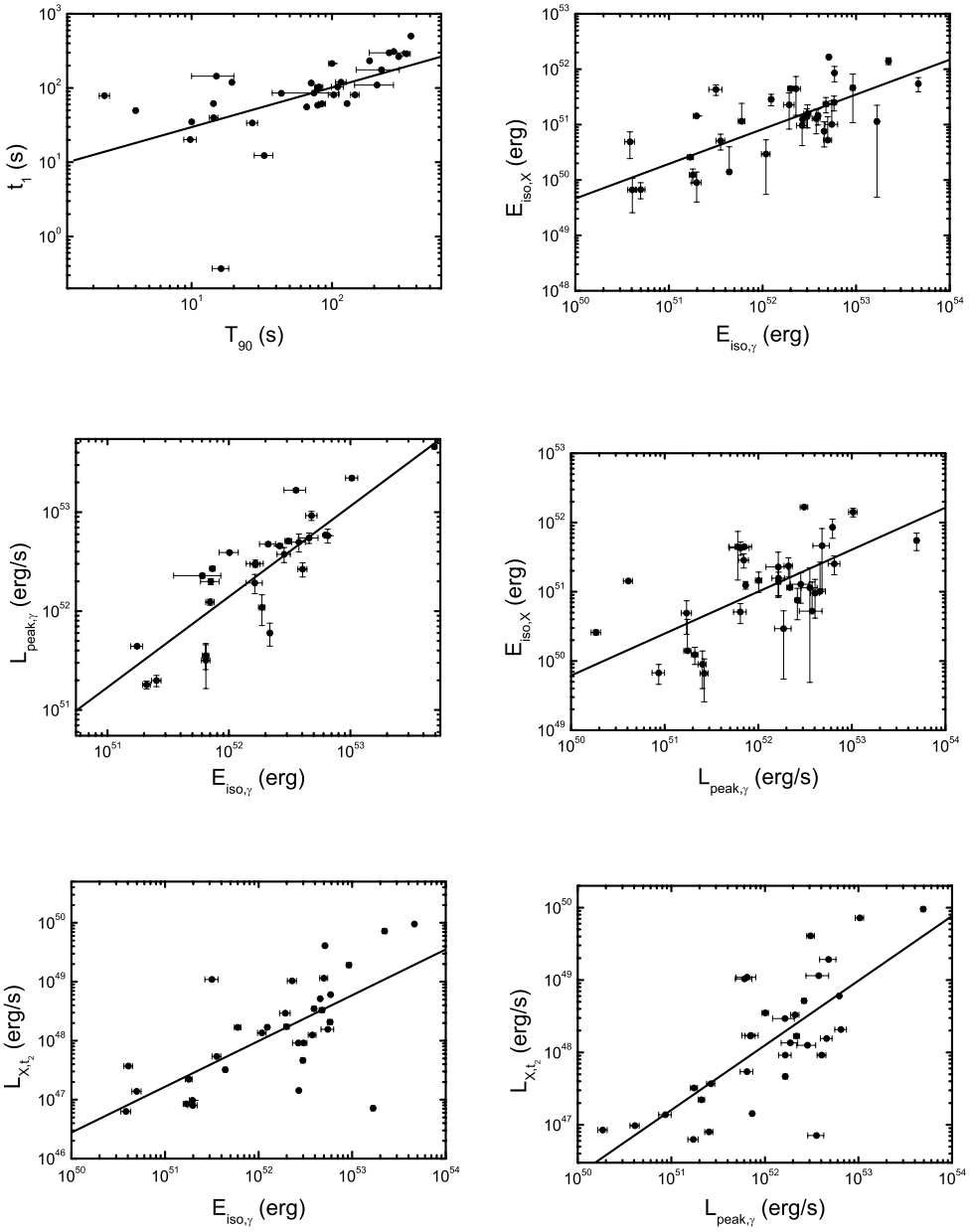

Figure 3. Correlation between the properties of the prompt gamma-ray phase and the shallow decay phase. Lines are the best-fitting results.

Table 2. Spearman correlation coefficients between the prompt gamma-rays and the X-rays in the shallow decay phase.

	t_1	$t_2 - t_1$	$t_3 - t_2$	L_{X,t_2}	$E_{\mathrm{iso,X}}$
T_{90}	0.55 (8.1E-4)[a]	0.58 (2.9E-4)	0.08 (0.63)	0.27 (0.13)	0.46 (6.3E-3)
$L_{\mathrm{peak},\gamma}$	0.40 (0.02)	0.08 (0.66)	−0.30 (0.08)	0.74 (<1E-4)	0.66 (<1E-4)
$E_{\mathrm{iso},\gamma}$	0.51 (2.2E-3)	0.33 (0.06)	−0.18 (0.31)	0.68 (<1E-4)	0.72 (<1E-4)

[a]In the bracket is the chance probability.

where α_{vis} is the viscous parameter and t_{acc} is the viscous accretion time-scale of the fall-back material. Please note that the time-scale T_{acc} is different from t_{acc} as $t_{\mathrm{acc}} \sim 2/\alpha_{\mathrm{vis}}\ \Omega_k$ is the viscous accretion time of the fall-back material after it has circularized but T_{acc} is the accretion time for fall-back material within different layers of the progenitor star, which is given by the fall-back time without considering the viscosity among the particles. Assuming that the observed flux is proportional to the accretion rate and that the time-scale t_{du} of the decrease of mass fall-back rate from f_2 to f_1 is much larger than t_{acc}, the upper limit of $f_\Omega(r)$ can be obtained by (Kumar

Table 3. Inferred properties of the progenitor stars for the bursts in our sample.

GRB	r_c[a] (10^9 cm)	r_t[a] (10^{10} cm)	r_e[a] (10^{11} cm)	$f_{\Omega,c}$[b]	$f_{\Omega,e,low}$[c] (10^{-3})	δ[d]	M_c[e] $M_\odot$	M_e[f] $0.1\,M_\odot$
050416A	9.14	0.98	0.72	[0.21 0.02]	7.85	2.56	0.02	0.04 ± 0.02
050803	2.15 ± 1.57	2.26 ± 0.27	3.16	[0.34 0.02]	3.75	2.04	0.09 ± 0.01	0.14 ± 0.01
050908	6.34 ± 3.53	2.03 ± 0.49	1.05	[0.19 0.03]	6.52	3.02	0.61 ± 0.06	0.16 ± 0.13
051016B	6.05 ± 1.30	1.30 ± 0.23	7.34	[0.29 0.03]	2.46	1.71	0.02 ± 0.01	0.27 ± 0.14
051109A	4.86 ± 2.50	0.97 ± 0.32	1.17	[0.33 0.03]	6.16	2.13	0.18 ± 0.03	2.38 ± 0.51
060108	3.87 ± 3.23	1.08 ± 0.33	2.62	[0.34 0.03]	4.12	2.09	0.20 ± 0.02	0.28 ± 0.09
060210	10.74 ± 0.93	1.42 ± 0.12	0.88	[0.30 0.02]	7.10	2.70	12.29 ± 0.66	7.81 ± 1.11
060418	7.09 ± 0.50	1.73 ± 0.10	0.38	[0.33 0.03]	10.83	1.50	2.53 ± 0.08	0.42 ± 0.20
060502A	2.01 ± 1.29	1.25 ± 0.21	6.56	[0.24 0.05]	2.60	2.39	0.69 ± 0.03	1.59 ± 0.37
060510B	9.76 ± 0.32	4.64	6.54	[0.38 0.02]	2.61	1.50	9.27 ± 0.40	0.63 ± 0.60
060522	4.98 ± 1.28	0.82 ± 0.13	0.17	[0.33 0.03]	16.26	1.50	2.77 ± 0.27	0.29 ± 0.47
060526	11.04 ± 0.30	2.71 ± 0.18	1.24	[0.35 0.02]	5.99	1.50	1.47 ± 0.19	0.53 ± 0.30
060605	3.70 ± 4.30	1.45 ± 0.30	0.90	[0.36 0.03]	7.05	1.50	1.07 ± 0.14	1.26 ± 0.80
060607A	9.76 ± 1.46	1.44 ± 0.13	1.46	[0.34 0.02]	5.53	2.15	2.84 ± 0.11	9.23 ± 0.19
060707	3.76 ± 2.02	1.64 ± 0.46	1.20	[0.31 0.03]	6.09	2.09	2.08 ± 0.20	0.71 ± 0.33
060708	2.33 ± 0.57	1.18 ± 0.23	1.11	[0.24 0.04]	6.32	2.09	0.33 ± 0.03	0.64 ± 0.71
060714	8.01 ± 0.76	1.33 ± 0.18	0.69	[0.33 0.02]	8.00	1.53	2.65 ± 0.18	1.31 ± 0.41
060729	12.71 ± 0.91	2.95 ± 0.20	9.12	[0.29 0.02]	2.21	1.91	0.11 ± 0.01	0.79 ± 0.03
060814	8.68 ± 2.55	4.53 ± 0.82	3.12	[0.32 0.02]	3.78	1.72	1.50 ± 0.02	0.69 ± 0.09
060906	4.80 ± 2.21	0.91 ± 0.19	1.42	[0.31 0.03]	5.59	1.99	3.22 ± 0.20	1.40 ± 0.42
061121	8.77 ± 0.61	1.25 ± 0.09	3.34	[0.33 0.02]	3.65	1.88	3.27 ± 0.05	4.75 ± 1.47
070110	4.82 ± 0.58	2.02 ± 0.22	2.32	[0.30 0.03]	4.38	1.75	1.11 ± 0.07	2.48 ± 0.16
070306	8.67 ± 0.54	2.51 ± 0.15	2.30	[0.31 0.02]	4.40	1.50	1.65 ± 0.09	0.78 ± 0.29
070318	9.03 ± 2.41	4.03 ± 0.61	0.74	[0.39 0.02]	7.77	1.50	0.25 ± 0.01	0.08 ± 0.01
070721B	10.95 ± 1.08	1.47 ± 0.23	0.96	[0.32 0.02]	6.80	2.43	5.13 ± 0.28	2.57 ± 1.96
071021	6.61 ± 0.42	1.43 ± 0.37	1.55	[0.33 0.03]	5.35	2.06	3.05 ± 0.47	0.56 ± 0.09
080310	19.39 ± 0.39	3.67	2.26	[0.37 0.02]	4.44	2.00	1.68 ± 0.15	0.87 ± 0.39
080430	0.25 ± 1.45	1.43 ± 0.25	2.03	[0.11 0.03]	4.68	2.28	0.10 ± 0.01	0.07 ± 0.02
080607	5.92 ± 0.38	1.05 ± 0.10	0.36	[0.34 0.03]	11.12	3.05	25.60	3.04 ± 0.86
080707	4.27 ± 1.60	1.36 ± 0.37	1.58	[0.32 0.03]	5.31	1.74	0.11 ± 0.01	0.05 ± 0.03
080905B	4.84 ± 0.96	0.98 ± 0.11	0.78	[0.37 0.03]	7.55	1.50	1.27 ± 0.14	2.47 ± 1.65
081007	5.61	1.72 ± 0.15	2.43	[0.25 0.03]	4.27	2.54	0.03 ± 0.01	0.04 ± 0.01
081008	12.74 ± 0.70	2.08 ± 0.21	1.56	[0.33 0.02]	5.33	2.60	2.18 ± 0.10	0.81 ± 0.26

[a]Radii of the core, transit and envelope region of the progenitor stars.
[b]The range of the rotational parameter of the core layer, $f_\Omega \equiv \frac{\Omega}{\Omega_k}$.
[c]The lower limit on the rotational parameter of the envelope layer.
[d]The density profile in the stellar envelope: $\rho(r) \sim r^{-\delta}$.
[e]The fall-back mass during the prompt phase.
[f]The fall-back mass during the shallow decay phase.

et al. 2008a,b)

$$\left(\frac{t_{\rm du}}{t_{\rm acc}}\right)^2 \geq \frac{f_2}{f_1}. \quad (5)$$

A lower limit on $f_\Omega(r)$ is derived from the centrifugally supporting condition that the fall-back material is able to form an accretion disc at a radius $r_{\rm d} \approx r[f_\Omega(r)]^2$, i.e. $r_{\rm d} \geq 3R_{\rm g}$, where $R_{\rm g} \equiv GM_{\rm BH}/c^2$ (c is the velocity of the light). For a convective envelope, the density profile at r is $\rho \propto r^{-\delta}$, where δ is determined by the slope of the shallow decay segment, with $\delta = 3(\alpha_2 + 1)/2$. The sharp decline in the steep decay indicates that the density in the transition region decreases sharply. In this region, $t_{\rm acc} \gg t_{\rm du}$, so the accretion in this region can be ignored.

With the data of the bursts in our sample, we calculate the radii for stellar core $r_{\rm c}$, transient region r_t, envelope region $r_{\rm e}$, the limits of spin parameter f_Ω, the index of the density profile δ, the accreted masses ($M_{\rm c}$ and $M_{\rm e}$) and the average accretion rates ($\dot{M}_{\rm c}$ and $\dot{M}_{\rm e}$) in the prompt gamma-ray and the shallow decay phases. They are tabulated in Table 3. We show the distributions of these parameters in Fig. 4. We find that the derived radii of the core layers of the progenitor stars for all the bursts are $r_{\rm c} = 10^9 \sim 10^{10}$ cm with the rotation parameter as $f_{\Omega,c} = 0.02 \sim 0.05$. The masses of the core layers for about two-thirds of GRBs in our sample are $M_{\rm c} = 0.1 \sim 5\,{\rm M}_\odot$ with a mass density of $10^2 \sim 10^5$ g cm^{-3}, and their average accretion rates in the prompt gamma-ray phase are $\dot{M}_{\rm c} = 0.01 \sim 1\,{\rm M}_\odot\,{\rm s}^{-1}$.

For the envelope layer, the estimated radii, lower limits on the rotation parameters and the masses of the fall-back materials are $r_{\rm e} = 10^{10} \sim 10^{12}$ cm, the lower limit for the rotation parameter $f_{\Omega,{\rm e}} = 10^{-3} \sim 10^{-2}$ and $M_{\rm e} = 10^{-3} \sim 1\,{\rm M}_\odot$, respectively. The average accretion rates in the shallow decay phase are much lower than that in the prompt gamma-ray phase, i.e. $\dot{M}_{\rm e} = 10^{-8} \sim 10^{-4}\,{\rm M}_\odot\,{\rm s}^{-1}$, but they are correlated. We measure the correlation with the Spearman correlation analysis, which yields $\log \dot{M}_{\rm c} = (-4.03 \pm 0.21) + (0.78 \pm 0.14) \log \dot{M}_{\rm e}$ with a correlation coefficient $r = 0.72$ and a chance probability $p < 10^{-4}$, as shown in Fig. 5. The estimated mass density in the envelope is $\sim 10^{-4}$ g cm^{-3}.

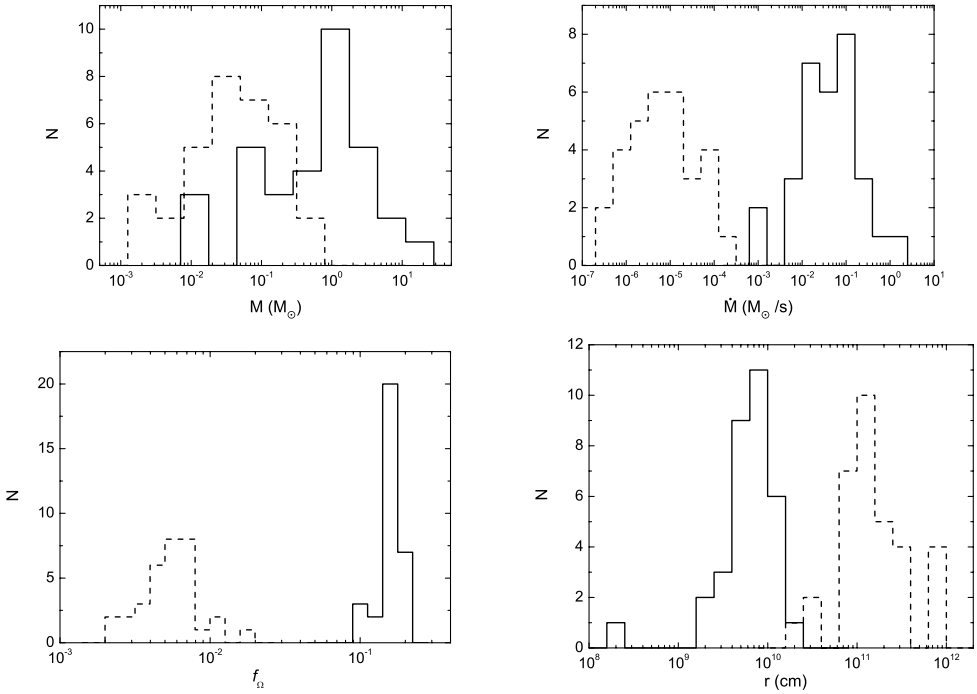

Figure 4. Distributions of the derived properties of the core (solid) and envelope (dashed) layers.

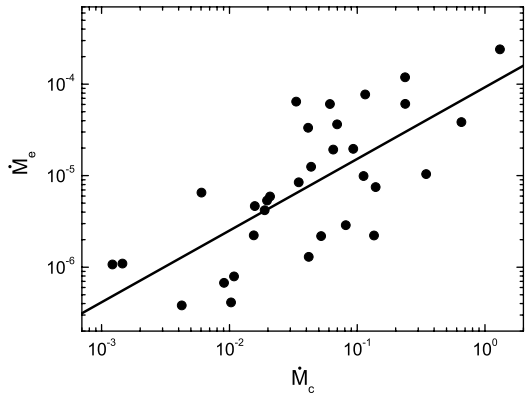

Figure 5. Correlation of the average accretion rates between the prompt gamma-rays $\dot{M}_c$ and the shallow decay phases $\dot{M}_e$. The solid line is the best-fit to the data with a Spearman correlation coefficient $r = 0.72$ and chance probability $p < 10^{-4}$.

5 CONCLUSIONS AND DISCUSSION

We have investigated the characteristics of the X-rays in the GRB rest frame, and inferred the properties of progenitor stars with a sample of 33 GRBs based on the model of Kumar et al. Assuming that the steep decay segment is due to the curvature effect, we fit the light curves with a broken power-law to derive the zero time of the last emission epoch of the prompt emission (t_1), the beginning (t_2) and the end time (t_3) of the shallow decay segment. The T_{90} is roughly consistent with t_1, but it is not correlated with the time intervals of $t_2 - t_1$ and $t_3 - t_2$. The $E_{\rm iso,\gamma}$ and $L_{\rm peak,\gamma}$ are correlated with $E_{\rm iso,X}$ and $L_{{\rm X},t_2}$. This fact likely suggests that the energy budgets for the two phases may be from the same central engine.

Based on a model proposed by Kumar et al. (2008a,b), we inferred the properties of the progenitor star with both the prompt gamma-rays and the X-ray data. The derived radii of the core layers of the progenitor stars for all the bursts are $r_c = 10^8 \sim 10^{10}$ cm with a rotation parameter as $f_{\Omega,c} = 0.02 \sim 0.05$. The masses of the core layers for about two-thirds of GRBs in our sample are $M_c = 0.1 \sim 5\,{\rm M}_\odot$ with a mass density of $10^2 \sim 10^5$ g cm^{-3}, and their average accretion rates in the prompt gamma-ray phase are $\dot{M}_c = 0.01 \sim 1\,{\rm M}_\odot\,{\rm s}^{-1}$. The estimated radii, lower limits on the rotation parameters and the masses of the fall-back materials for the envelope layers are $r_e = 10^{10} \sim 10^{12}$ cm, $f_{\Omega,e} = 10^{-3} \sim 10^{-2}$ and $M_e = 10^{-3} \sim 1\,{\rm M}_\odot$, respectively. The average accretion rates in the shallow decay phase are much lower than those in the prompt gamma-ray phase, i.e. $\dot{M}_e = 10^{-8} \sim 10^{-4}\,{\rm M}_\odot\,{\rm s}^{-1}$, but they are correlated. The estimated mass density in the envelope is $\sim 10^{-4}$ g cm^{-3}.

The connection between long-duration GRBs and SNe was predicted theoretically (Colgate 1974; Woosley 1993) and has been verified observationally through detecting spectroscopic features of the underlying SNe in some nearby GRBs (Woosley & Bloom 2006). The collapsar model is the most promising scenario to explain the huge release of energy associated with long-duration GRBs (Woosley & Weaver 1995; Paczyński 1998; MacFadyen & Woosley 1999; Zhang, Kobayashi & Mészáros 2003; Janiuk & Proga 2008). In this scenario, GRBs are produced by a jet powered by accretion of the core and the fall-back materials of the progenitor star through a torus. We infer the properties of the progenitor stars by assuming that both the prompt gamma-rays and the X-rays observed with XRT are due to the accretion of different layers of progenitor stars. We compare the distribution of r_e, the radius of envelope region, with the photospheric radii of a sample with 25 WC-type and 61 WN-type Wolf–Rayet (WR) stars (Koesterke & Hamann 1995; Li 2007) in Fig. 6. We find that the photospheric radius of a WR star is larger than r_e, consistent with our prediction.

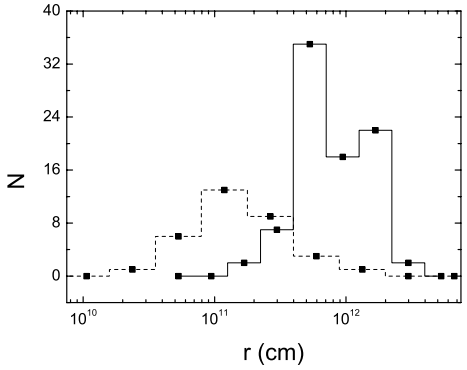

Figure 6. Comparison of the radii of the envelope layers of the bursts in our sample (step dash line) with the photospherical radii of 86 WR stars (step solid line).

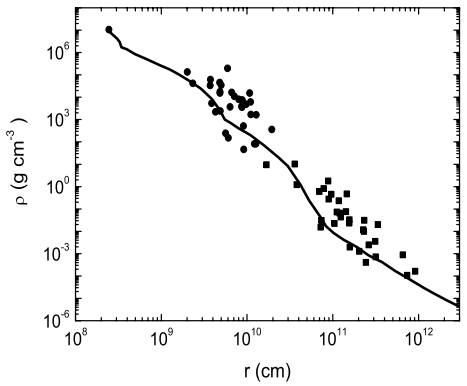

Figure 7. Assembled mass density as a function of radius for the bursts in our sample with comparison of the simulation for a pre-supernova star with mass of 25 $M_\odot$ (the curve).

In our calculation, we regard that all GRBs are from a unified collapsar with a central BH of $M = 10\,M_\odot$. Our results thus might be compared with simulation results for a collapsar with a given mass. We compare the derived mass density profile as a function of radius r with simulations in Fig. 7, in which the simulated mass density profile is taken from Woosley & Weaver (1995) for a massive star with $M = 25\,M_\odot$ (see also Janiuk & Proga 2008). It is found that, although the derived ρ are systematically larger than the results of simulations, they are very consistent with the simulations.

In the collapsar models, the accretion duration should be as long as the material fall-back time-scale from the collapsar envelope available to fuel the accretion disc or torus. Rotation of the progenitor star should be high enough to form the disc or torus. One thus might expect a relation between the burst duration and the rotation parameter f_Ω. For a progenitor star with higher rotation, the angular momentum loss should be longer, and the accretion time-scale might be longer, hence a longer GRB event. We show the correlation between t_1 and f_Ω in Fig. 8. A tentative correlation is found, with a correlation coefficient of 0.72 and a chance probability $p < 10^{-4}$. This correlation indicates that the higher f_Ω, the longer GRB could be observed, consistent with the model's expectation.

It is believed that GRBs are highly collimated, with a beaming factor $f_b \sim 1/500$ from the optical afterglow observations (Frail, Kulkarni & Sari 2001). The measurement of the beaming angle has also proven exceedingly difficult in the *Swift* era (Cenko et al. 2009). In our analysis, we do not consider the beaming effect. The lack of detection of jet-like breaks in the late XRT light curve might suggest that the X-ray jet would be less collimated than expected from the optical data (Burrows & Racusin 2006; Liang et al. 2008). In spite of this, the accretion rates and the accreted masses could be up to two orders of magnitude lower than those derived in this analysis if beaming is considered.

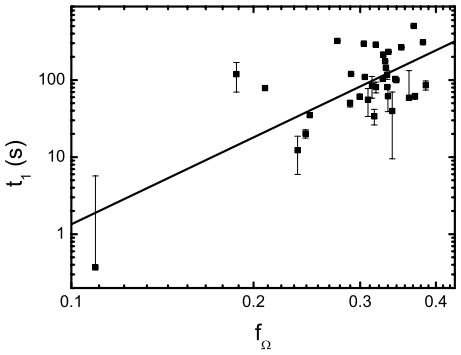

Figure 8. Correlation between the rotational parameter and the burst duration.

ACKNOWLEDGMENTS

We appreciate valuable suggestions and comments from the anonymous referee. We also thank Bing Zhang, Li-Xin Li, Zhuo Li and Tong Liu for helpful discussion.

REFERENCES

Burrows D. N., Racusin J., 2006, Nuovo Cimento B, 121, 1273
Cenko S. B. et al., 2009, ApJ, submitted (arXiv:0905.0690)
Chen W. X., Beloborodov A. M., 2007, ApJ, 657, 383
Colgate S. A., 1974, ApJ, 187, 333
Di Matteo T., Perna R., Narayan R., 2002, ApJ, 579, 706
Fan Y., Piran T., 2006, MNRAS, 369, 197
Frail D. A., Kulkarni S. R., Sari R., 2001, ApJ, 562, L55
Genet F., Daigne F., Mochkovitch R., 2007, MNRAS, 381, 732
Ghisellini G., 2008, in Huang Y.-F., Dai Z.-G., Zhang B., eds, AIP Conf. Proc. Vol. 1065, 2008 Nanjing Gamma-Ray Burst Conference. Am. Inst. Phys., New York, p. 137
Ghisellini G., Ghirlanda G., Nava L., Firmani C., 2007, ApJ, 658, L75
Gu W. M., Liu T., Lu J. F., 2006, ApJ, 643, L87
Ioka K., Kobayashi S., Zhang B., Kenji T., Yamazaki R., Nakamura T., 2006, in Holt S. S., Gehrels N., Nausek J. A., eds, AIP Conf. Proc. Vol. 836, Gamma-Ray Bursts in the Swift Era: Sixteenth Maryland Astrophysics Conference. Am. Inst. Phys., New York, p. 301
Janiuk A., Proga D., 2008, ApJ, 675, 519
Janiuk A., Yuan Y. F., Perna R., Di Matteo T., 2007, ApJ, 664, 1011
Kawanaka N., Mineshige S., 2007, ApJ, 662, 1156
Koesterke L., Hamann W. R., 1995, A&A, 299, 503
Kohri K., Mineshige S., 2002, ApJ, 577, 311
Kohri K., Narayan R., Piran T., 2005, ApJ, 629, 341
Kumar P., Panaitescu A., 2000, ApJ, 541, L51
Kumar P., Narayan R., Johnson J., 2008a, Sci, 321, 376
Kumar P., Narayan R., Johnson J., 2008b, MNRAS, 388, 1729
Lee W. H., Ramirez-Ruiz E., Page D., 2005, ApJ, 632, 421
Li L. X., 2007, MNRAS, 375, 240
Liang E. W., Zhang B., O'Brien P. T., 2006, ApJ, 646, 351
Liang E. W., Zhang B. B., Zhang B., 2007, ApJ, 670, 565
Liang E. W., Racusin J. L., Zhang B., Burrows D. N., 2008, ApJ, 675, 528

Liang E. W., Lv H. J., Zhang B. B., Zhang B., 2009, ApJ, in press (arXiv:0902.3504)
Liu T., Gu W. M., Xue L., Lu J. F., 2007, ApJ, 661, 1025
MacFadyen A. I., Woosley S. E., 1999, ApJ, 524, 262
McKinney J. C., 2005, ApJ, 630, L5
Mészáros P., 2006, Rep. Prog. Phys., 69, 2259
Narayan R., Piran T., Kumar P., 2001, ApJ, 557, 949
Nava L., Ghisellini G., Ghirlanda G., Cabrera J. I., Firmani C., Avila-Reese V., 2007, MNRAS, 377, 1464
Nousek J. A. et al., 2006, ApJ, 642, 389
O'Brien P. T. et al., 2006, ApJ, 647, 1213
Paczyński B., 1998, ApJ, 494, L45
Panaitescu A., 2007, MNRAS, 380, 374
Piran T., 2005, Rev. Mod. Phys., 76, 1143
Popham R., Woosley S. E., Fryer C., 1999, ApJ, 518, 356
Qin Y. P., 2008, ApJ, 683, 900
Qin Y. P., 2009, ApJ, 691, 811
Qin Y. P., Zhang Z. B., Zhang F. W., Cui X. H., 2004, ApJ, 617, 439
Racusin J. L. et al., 2009, ApJ, 698, 43
Shao L., Dai Z. G., 2007, ApJ, 660, 1319
Shen R.-F., Kumar P., Robinson E. L., 2006, MNRAS, 371, 1441
Shen R.-F., Willingale R., Kumar P., O'Brien P. T., Evans P. A., 2009, MNRAS, 393, 598
Troja E. et al., 2007, ApJ, 665, 599
Uhm Z. L., Beloborodov A. M., 2007, ApJ, 665L, 93
Willingale R. et al., 2007, ApJ, 662, 1093
Woosley S. E., 1993, ApJ, 405, 273
Woosley S. E., Bloom J. S., 2006, ARA&A, 44, 507
Woosley S. E., Weaver T. A., 1995, ApJS, 101, 181
Yamazaki R., 2009, ApJ, 690, L118
Zhang B., 2007, Chin. J. Astron. Astrophys., 7, 1
Zhang B., Mészáros P., 2004, Int. J. Mod. Phys. A, 19, 2385
Zhang B., Kobayashi S., Mészáros P., 2003, ApJ, 595, 950
Zhang B., Fan Y. Z., Dyks J., Kobayashi S., Mészaros P., Burrows D. N., Nousek J. A., Gehrels N., 2006, ApJ, 642, 354
Zhang B. et al., 2007a, ApJ, 655, 989
Zhang B. B., Liang E. W., Zhang B., 2007b, ApJ, 666, 1002
Zhang B. B., Zhang B., Liang E. W., Wang X. Y., 2009, ApJ, 690, 10

This paper has been typeset from a TEX/LATEX file prepared by the author.